A Monte Carlo Study of Line Formation of Raman Scattered He II in an Expanding Spherical Shell

Bo-Eun Choi[1], Seok-Jun Chang[1,2], Hee-Won Lee[1]
[1]Department of Physics and Astronomy, Sejong University, [2]Korea Astronomy and Space Science Institute

Abstract

We investigate line formation of Raman-scattered He II in a thick H I region in order to study the mass loss processes in young planetary nebula. A new Monte-Carlo code to trace far UV He II photons that are transferred through Rayleigh and Raman scattering. The code incorporates a grid-based algorithm that can be flexibly applied to a situation where the neutral region is non-uniform and non-stationary. In our model, a hot He II emission source is placed at the center surrounded by a neutral region that is expanding in a spherically symmetrical way. We obtain significantly distorted multiply peaked profiles with Raman conversion efficiency increasing with the expansion speed of the neutral shell. We also find that the profiles have an extended red tail or an additional broad red shoulder that results from a combination of final Raman scattering and a few Rayleigh reflections at the inner surface of the neutral shell. These complicated features are attributed to sharp increase of scattering cross section toward resonance as well as the kinematics of the neutral region.

Introduction

Planetary Nebulae

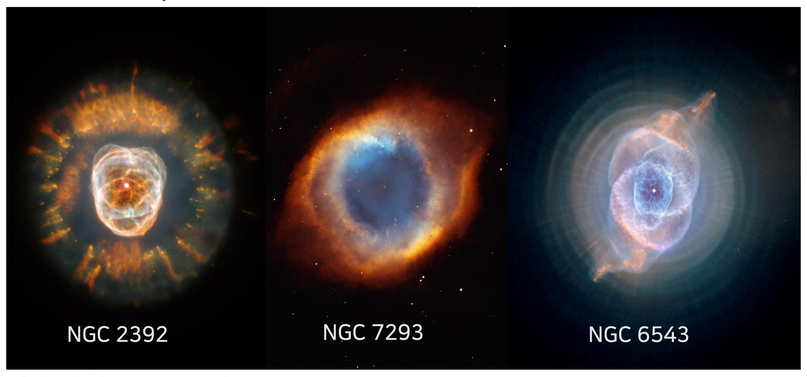

Fig 1. HST image of planetary nebulae.

- Low to intermediate mass stars (1-8$M_\odot$) lose their mass via heavy stellar winds while they are in the AGB stage.
- Investigation of neutral components is a key to understanding the mass loss process in AGB stage and formation of PNe.
- A powerful tool to examine the neutral region of PNe is spectral features formed through Raman scattering of He II with H I. These features appear blueward of Balmer lines.
- When He II UV photons are incident on the thick H I region, they can be transferred via Rayleigh and Raman scattering.
- Raman scattered features are found in NGC 7027, NGC 6302, IC 5117, and NGC 6790(Pequignot et al. 1997; Groves et al. 2002; Lee et al. 2006; Kang et al. 2009).

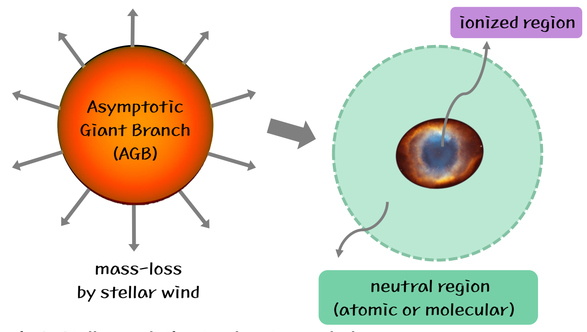

Fig 2. Stellar evolution to planetary nebula.

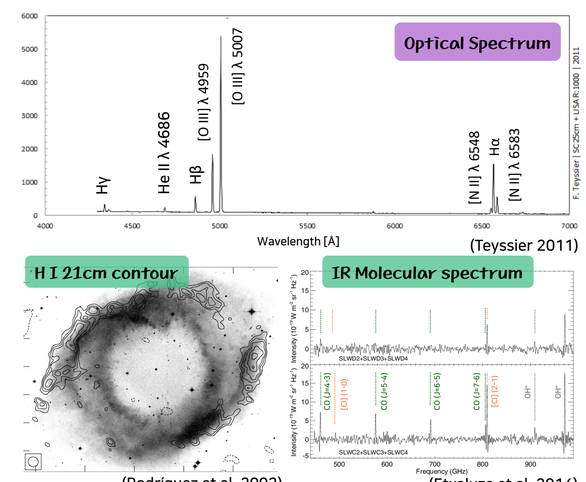

Fig 3. (Top) Optical spectrum of NGC 2392. (Bottom) H I 21cm lines and molecular lines(IR) from circumnebular neutral region of NGC 7293.

Raman Scattered He II λ4851

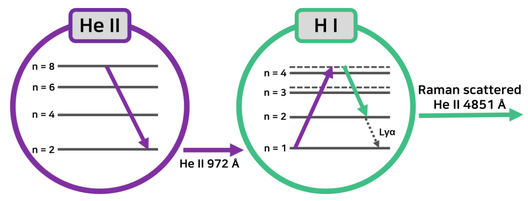

Fig 4. Schematic illustration of Raman scattering process.

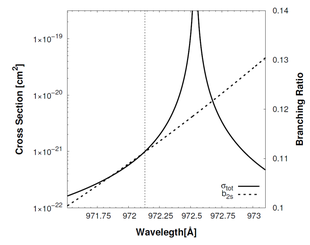

Fig 5. Cross section near Lyγ and the branching ratio to level n=2.

- **Kramers-Heisenberg formula**

$$\frac{d\sigma}{d\Omega} = r_e^2 \left(\frac{\omega'}{\omega}\right) \left| \delta_{AB}\left(\boldsymbol{\epsilon}^{(\alpha)} \cdot \boldsymbol{\epsilon}^{(\alpha')}\right) + \frac{1}{m_e} \sum_I \left(\frac{\left(\boldsymbol{p} \cdot \boldsymbol{\epsilon}^{(\alpha\prime)}\right)_{BI} \left(\boldsymbol{p} \cdot \boldsymbol{\epsilon}^{(\alpha)}\right)_{IA}}{E_I - E_A - \hbar\omega} + \frac{\left(\boldsymbol{p} \cdot \boldsymbol{\epsilon}^{(\alpha)}\right)_{BI} \left(\boldsymbol{p} \cdot \boldsymbol{\epsilon}^{(\alpha')}\right)_{IA}}{E_I - E_A + \hbar\omega'} \right)^2$$

- Cross section is given as an infinite sum over bound np states and integral over free n'p states.
- Cross section increases sharply as the wavelength approaches the line resonance.
- Raman features are excellent probes of thick H I components in mass losing objects in the presence of far UV illumination.

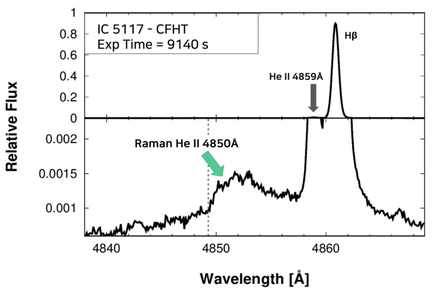

Fig 6. Spectrum of young planetary nebula IC 5117 around Hβ obtained with CFHT.

Scattering Geometry

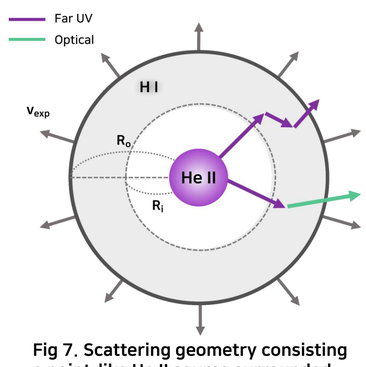

Fig 7. Scattering geometry consisting a point-like He II source surrounded by a neutral hydrogen shell.

- He II emission source is surrounded by a spherical shell-like neutral medium.
- The H I medium is moving away from the He II source with constant speed v_{exp}.
- He II photons can escape from the neutral region through Rayleigh and Raman scattering.
- The scattering geometry is parametrized with v_{exp} and H I column density given by

$$N_{HI} = \int_{R_i}^{R_o} n_{HI}(r) dr \,,$$

where $n_{HI}(r) = \frac{\dot{M}}{4\pi r^2 m_p v_{exp}}$, and $\dot{M}$ is mass loss rate.

Grid-based Numerical Radiative Transfer

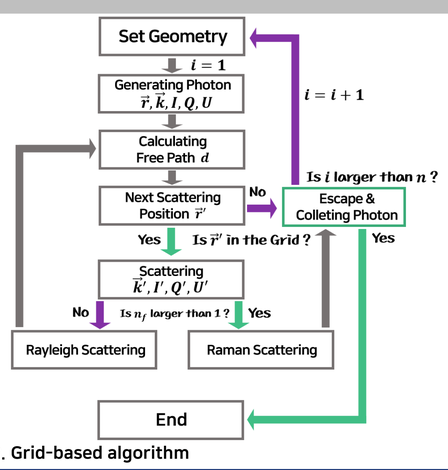

Fig 8. Grid-based algorithm

Assignment of Doppler factors : In the rest frame of the hydrogen atom, we assume that incident and outgoing far UV photons have the same frequency in the case of Rayleigh scattering.

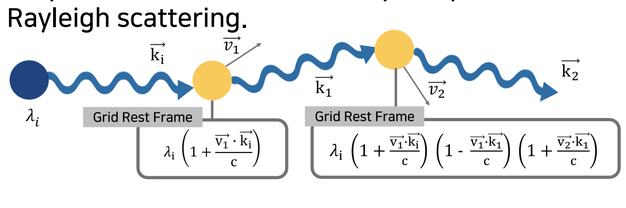

$\lambda_i \left(1 + \frac{\vec{v_1} \cdot \vec{k_i}}{c}\right)\left(1 - \frac{\vec{v_1} \cdot \vec{k_1}}{c}\right)$

$\lambda_i \left(1 + \frac{\vec{v_1} \cdot \vec{k_i}}{c}\right)\left(1 - \frac{\vec{v_1} \cdot \vec{k_1}}{c}\right)\left(1 + \frac{\vec{v_2} \cdot \vec{k_1}}{c}\right)\left(1 - \frac{\vec{v_2} \cdot \vec{k_2}}{c}\right)$

Fig 9. Wavelength changes during scattering process in grid-rest frame and observer's frame

Results

Monochromatic Source

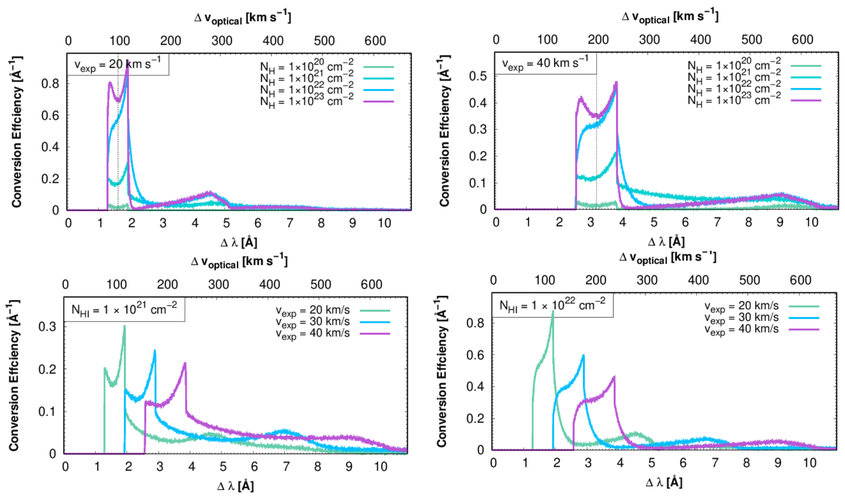

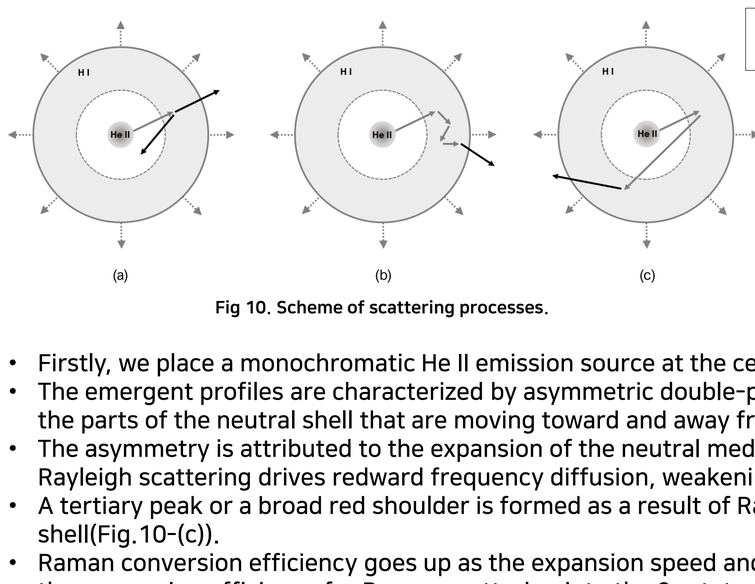

Fig 10. Scheme of scattering processes.

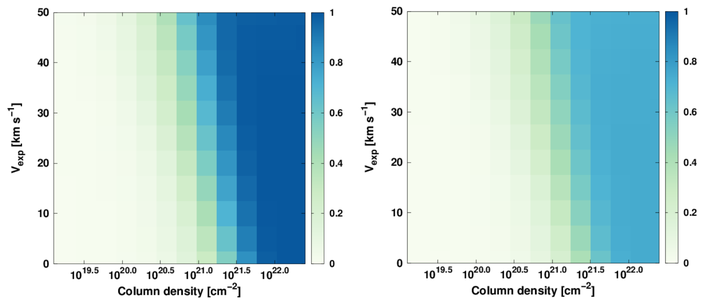

Fig 11. Raman conversion efficiency maps. (Left) Total Raman conversion efficiency. (Right) Raman conversion efficiency for Raman scattering into n=2.

- Firstly, we place a monochromatic He II emission source at the center of the neutral spherical shell.
- The emergent profiles are characterized by asymmetric double-peak structure, where the two peaks correspond to the Doppler factors of the parts of the neutral shell that are moving toward and away from the observer(Fig.10-(a)).
- The asymmetry is attributed to the expansion of the neutral medium because the hydrogen atoms move away from each other and multiple Rayleigh scattering drives redward frequency diffusion, weakening the blue peak part(Fig.10-(b)).
- A tertiary peak or a broad red shoulder is formed as a result of Rayleigh reflections at the inner boundary of the spherical neutral shell(Fig.10-(c)).
- Raman conversion efficiency goes up as the expansion speed and column density. In particular, the total efficiency converges to unity and the conversion efficiency for Raman scattering into the 2s state converges to the branching ratio determined by quantum mechanics.

Gaussian Source

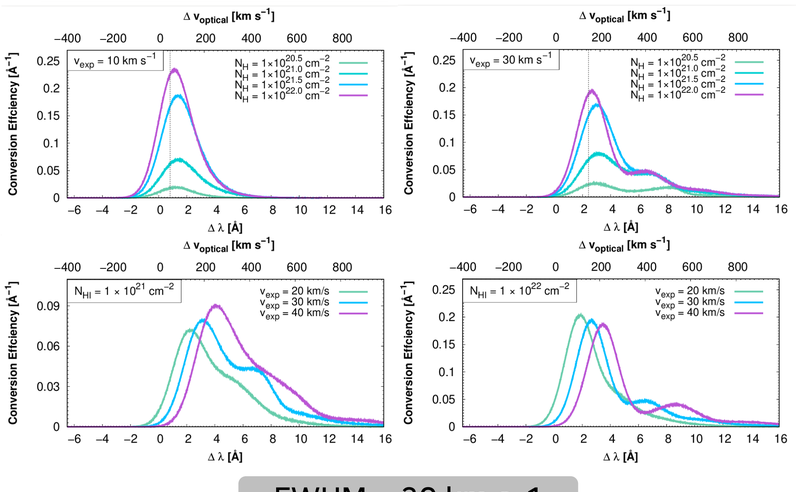

FWHM = 30 km s-1

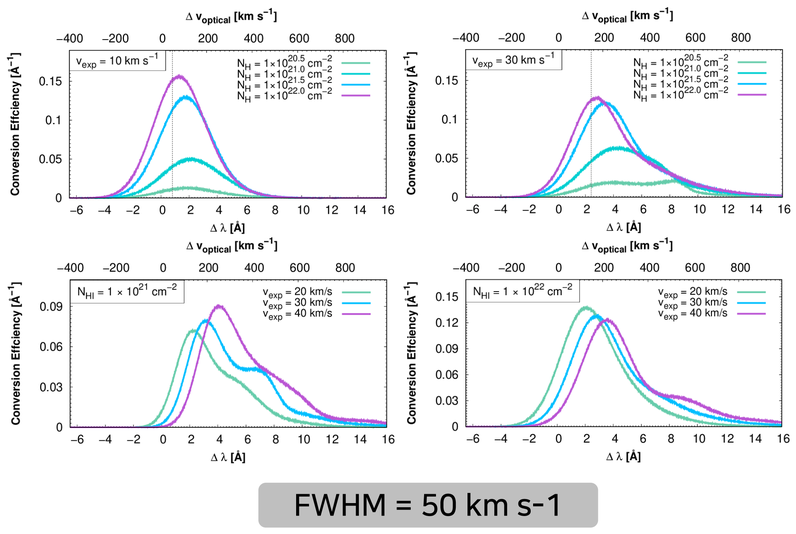

FWHM = 50 km s-1

- Secondly, we place a He II emission source with a Gaussian line profile at the center.
- The overall emergent profiles are dominantly single peaked. However, significant distortion in the emergent profiles are observed.
- Depending on the expansion speed and H I column density, there appears a red peak. This is due to enhanced cross section toward resonance that drives frequency diffusion.
- There are cases where the red peak dominates the central peak formed near atomic line center. This clearly illustrates the importance of atomic physics in line formation of Raman He II features.

Discussion

- We find significant redward frequency diffusion in line formation of Raman-scattered He II features in an expanding neutral shell.
- Raman conversion efficiency increases considerably as both the expansion speed and H I column density are increased.
- There appear prominent red extended tail or tertiary red peak as a result of sharply increasing cross section as line photons get redshifted.
- It is suggested that different parts of the Raman-scattered He II profile are characterized by differing scattering numbers.
- We will extend the current work to the cylindrical shell that is consistent with bipolar structures often seen in a large number of PNe including linear polarization.

Fig 10. Bipolar morphology of PNe.